

# Universal fit to $p$ - $p$ elastic diffraction scattering from the Lorentz-contracted geometrical model

P. H. Hansen and A. D. Krisch\*

*The Niels Bohr Institute, University of Copenhagen, DK-2100 Copenhagen, Denmark*

(Received 23 February 1977)

We examine the prediction of the Lorentz-contracted geometrical model for proton-proton elastic scattering at small angles. The model assumes that when two high-energy particles collide, each behaves as a geometrical object which has a Gaussian density and is spherically symmetric except for the Lorentz contraction in the incident direction. It predicted that  $d\sigma/dt$  should be independent of energy when plotted against the variable  $\beta^2 P_1^2 \sigma_{\text{tot}}(s)/(38.3 \text{ mb})$ . Thus the energy dependence of the diffraction-peak slope ( $b$  in an  $e^{-bt}$  plot) is given by  $b(s) = A^2 \beta^2 \sigma_{\text{tot}}(s)/(38.3 \text{ mb})$ , where  $\beta$  is the proton's c.m. velocity and  $A$  is its radius. We used recently measured values of  $\sigma_{\text{tot}}(s)$ , and obtained an excellent fit to the elastic slope in both  $t$  regions [ $-t < 0.1 \text{ (GeV/c)}^2$  and  $0.1 < -t < 0.4 \text{ (GeV/c)}^2$ ] at all energies from  $s = 6$  to  $4000 \text{ (GeV)}^2$ .

Recent measurements of hadronic scattering cross sections at the CERN ISR and at Fermilab have given considerable support to geometrical models for very-high-energy scattering. The basic assumption of all geometrical models is that hadrons are objects with a size of about 1 Fermi and that this size determines many properties of the scattering cross sections. Such models have been studied for many years. Serber's<sup>1</sup> optical model for elastic scattering was probably the first geometrical model and it was soon followed by the models of Krisch,<sup>2</sup> Van Hove,<sup>3</sup> Wu and Yang,<sup>4</sup> Durand and Lippe,<sup>5</sup> and many others. Models with at least some geometrical aspects have been applied to inclusive reactions by Van Hove,<sup>3</sup> Krisch,<sup>2,6,7</sup> Huang,<sup>8</sup> Yang *et al.*,<sup>9</sup> Feynman,<sup>10</sup> and others.<sup>11</sup> The geometrical nature of Feynman's prediction that  $E d^3\sigma/dP^3$  would be energy-independent when plotted against  $x$  and  $P_1$  has been discussed earlier.<sup>7,12</sup>

In this paper we will examine the Lorentz-contracted geometrical model's prediction about the "shrinkage" of the  $p$ - $p$  elastic diffraction peak. In 1966 Krisch<sup>6</sup> suggested that the  $p$ - $p$  elastic cross section should depend only on the variable  $\beta^2 P_1^2$ . The slope  $b$  in an  $e^{-bt}$  plot should then be proportional to  $\beta^2$ , where  $\beta = v/c$  is the c.m. velocity of each proton. In fact the proton-proton elastic cross section was predicted to have the form

$$\frac{d\sigma^+}{dt} = 90e^{-1.0\beta^2 P_1^2} + 0.74e^{-3.45\beta^2 P_1^2} + 0.0029e^{-1.45\beta^2 P_1^2} \quad (1)$$

(where  $d\sigma^+/dt$  is in  $\text{mb}/(\text{GeV}/c)^2$  and  $P_1$  is in  $\text{GeV}/c$ ), a universal curve in the variable  $\beta^2 P_1^2$  with three distinct regions corresponding to three spatial regions with different sizes. This curve fitted all data available at that time.

Leader and Pennington<sup>13</sup> and others<sup>14</sup> have shown that in the diffraction peak this prediction was fairly well verified by ISR and Fermilab data. However, Mellissinos and Olsen<sup>15</sup> have pointed out that there was some deviation above  $s = 1000 \text{ (GeV)}^2$ . Equation (1) also predicted the large- $\beta^2 P_1^2$  behavior of  $p+p \rightarrow p+p$ . Major deviations were first found by Allaby *et al.*<sup>16</sup> in the range  $\beta^2 P_1^2 = 1-3 \text{ (GeV/c)}^2$ . These deviations were discussed by Giacomelli.<sup>17</sup> In fact it now appears that the second region of this model, the  $e^{-3.45\beta^2 P_1^2}$  term, may be due to potential scattering rather than diffraction scattering and that it may fall as  $1/s$  and thus disappear at ISR energies.

There are additional problems at large angles due to particle-identity effects near  $90^\circ$ . The dagger in Eq. (1) refers to an attempt to deal with these.<sup>6</sup> However, they are very sensitive to the spin dependence of  $p$ - $p$  elastic scattering, which is apparently quite significant at large  $P_1^2$  up to  $12 \text{ GeV}/c$ .<sup>18</sup> We will thus concentrate here on the diffraction peak and study the large- $\beta^2 P_1^2$  behavior later.

More recently Krisch<sup>12</sup> proposed modifying the variable from  $\beta^2 P_1^2$  to

$$\beta^2 P_1^2 \frac{\sigma_{\text{tot}}(s)}{\sigma_{\text{tot}}(\infty)}. \quad (2)$$

This modification allows for the energy dependence of the radius associated with a changing  $\sigma_{\text{tot}}(s)$ . This explained much of the energy dependence of the diffraction-peak slopes in  $\pi^\pm$ - $p$ ,  $K^\pm$ - $p$ , and  $p$ - $\bar{p}$  elastic scattering. For some of these reactions  $\sigma_{\text{tot}}$  was already known to have a strong energy dependence. At that time it was generally believed that, above  $s = 40 \text{ (GeV)}^2$ ,  $\sigma_{\text{tot}}(p-p)$  was energy independent and equal to about 38.8 mb. Thus the formula given for the  $p$ - $p$  elastic slope ( $b$  in  $e^{-bt}$ )

$$b(s) = 10.5\beta^2 \frac{\sigma_{\text{tot}}(s)}{38.8 \text{ mb}} \quad (3)$$

did not exactly fit when  $\sigma_{\text{tot}}(s)$  was taken to be 38.8 mb at  $s$  above 1000  $(\text{GeV})^2$ . We now know that  $\sigma_{\text{tot}}(s)$  grows with increasing energy and that this growth may cause some of the "shrinkage" of the elastic slope. This relation between  $\sigma_{\text{tot}}$  and slope has been stressed recently by Dias de Deus *et al.*<sup>19</sup> under the name of geometric scaling.

The Lorentz-contracted geometric model thus predicts that  $d\sigma/dt$  should behave as

$$\frac{d\sigma}{dt} = \frac{\sigma_{\text{tot}}^2}{16\pi} \left\{ \sum_i a_i \exp \left[ -A_i^2 \beta^2 P_{\perp}^2 \frac{\sigma_{\text{tot}}(s)}{\sigma_{\text{tot}}(s_0)} \right] \right\}. \quad (4)$$

Since  $\sigma_{\text{tot}}(s)$  increases with energy, its value at  $s = \infty$  is clearly unknown. Thus we must choose some other  $s_0$  where  $\sigma_{\text{tot}}$  is well measured. In Fig. 1 are plotted the measured values<sup>20-26</sup> of  $\sigma_{\text{tot}}$  for proton-proton scattering. We choose  $s_0 = 100 (\text{GeV})^2$  near the minimum where  $\sigma_{\text{tot}}$  is taken to be 38.3 mb.

Since most experimenters plot their elastic differential cross sections against  $t$ , it is useful to relate  $t$  to our variable which we will call  $\rho_{\perp}^2$

$$\begin{aligned} t &= -2P_{\text{c.m.}}^2 (1 - \cos \theta_{\text{c.m.}}), \\ \rho_{\perp}^2 &= \beta^2 P_{\perp}^2 \frac{\sigma_{\text{tot}}(s)}{38.3} \\ &= \beta_{\text{c.m.}}^2 P_{\text{c.m.}}^2 \sin^2 \theta_{\text{c.m.}} \frac{\sigma_{\text{tot}}(s)}{38.3}. \end{aligned} \quad (5)$$

Some useful relations are

$$\rho_{\perp}^2 = \frac{tu}{s} \frac{\sigma_{\text{tot}}(s)}{38.3}, \quad (6)$$

$$\rho_{\perp}^2 = \beta^2 |t| \left( 1 - \frac{|t|}{s - 4m^2} \right) \frac{\sigma_{\text{tot}}(s)}{38.3}.$$

These allow one to directly calculate  $\rho_{\perp}^2$  for each data point when  $s$  and  $t$  are given.

We will first calculate the energy dependence of the slope  $b$  in a conventional  $t$  plot. In the diffraction peak  $d\sigma/dt$  is assumed to have the energy-independent form of Eq. (4)

$$\frac{d\sigma}{dt} \propto \exp \left[ -A^2 \beta^2 P_{\perp}^2 \frac{\sigma_{\text{tot}}(s)}{38.3} \right]. \quad (7)$$

The slope of a  $t$  plot is by definition

$$b(s) = \frac{d}{dt} \left[ \ln \left( \frac{d\sigma}{dt} \right) \right]. \quad (8)$$

Substituting Eq. (6) into Eq. (7) and differentiating, we obtain

$$b(s) = A^2 \beta^2 \frac{\sigma_{\text{tot}}(s)}{38.3 \text{ mb}} \left( 1 - \frac{2\langle t \rangle}{s - 4m^2} \right), \quad (9)$$

where  $\langle t \rangle$  is the average value of  $|t|$ . The final term comes from the kinematic difference between the variables  $t$  and  $P_{\perp}^2$ . At high  $s$  this term is very close to 1 for small  $t$ . For example at  $s = 100 (\text{GeV})^2$  and  $|t| = 0.1 (\text{GeV}/c)^2$  it equals 0.999. However, at larger angles the factor is quite significant; in fact at  $90^\circ$   $|t| = 2P_{\perp}^2$  and  $b(s)$  is exactly zero.

In addition to the three regions of Eq. (1) it is

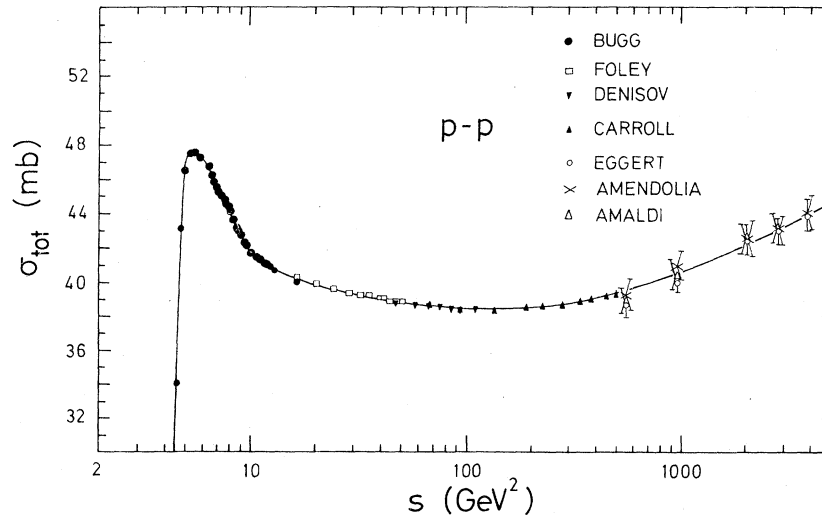


FIG. 1. The measured values of  $\sigma_{\text{tot}}$  for proton-proton scattering are plotted against  $s$ . The curve is a smooth hand-drawn fit to the data. The corresponding values of  $\sigma_{\text{tot}}/38.3 \text{ mb}$  are given in Table I.

now well known that there is another very forward region in the  $p$ - $p$  elastic diffraction peak. This was first suggested by Carrigan.<sup>27</sup> The two regions in the diffraction peak are approximately given by

$$\frac{d\sigma}{dt} \propto \begin{cases} e^{-12|t|}, & -t < 0.1 \text{ (GeV/c)}^2 \\ e^{-10.5|t|}, & 0.1 < -t < 0.4 \text{ (GeV/c)}^2 \end{cases} \quad (10)$$

at high energy. The conventional  $t$ -plot slopes in these two regions are given by Eq. (9) to be

$$b(s) = \begin{cases} 11.35\beta^2 \frac{\sigma_{\text{tot}}(s)}{38.3 \text{ mb}} \left(1 - \frac{0.1}{s - 4m_p^2}\right) (\text{GeV/c})^{-2}, & -t < 0.1 \text{ (GeV/c)}^2 \\ 10.05\beta^2 \frac{\sigma_{\text{tot}}(s)}{38.3 \text{ mb}} \left(1 - \frac{0.5}{s - 4m_p^2}\right) (\text{GeV/c})^{-2}, & 0.1 < -t < 0.4 \text{ (GeV/c)}^2. \end{cases} \quad (11)$$

We have taken 0.10 and 0.50 to be twice the average value of  $|t|$  in each region. The parameters 11.35 and 10.05 were chosen to fit the data. They correspond to sizes of about 1 F and 0.9 F.

In Figs. 2 and 3 we plot Eq. (11) along with the experimentally measured slopes<sup>28</sup> for proton-proton elastic scattering at various energies. We have plotted all data we could find in compilations<sup>29,30</sup> or in the recent literature,<sup>31-56</sup> except that we excluded the old low-energy data with large errors which were specifically excluded by the authors of a compilation.<sup>29</sup> In general the fit looks quite good. However, the quality of the fit is somewhat obscured by significant disagreements between different experiments at nearby  $s$  values. This disagreement is not surprising as the plot represents many different experiments done during the past 20 years using very different techniques.

To improve the test of the model, we averaged

different measurements at nearby energies. This removed some of the systematic errors. We typically grouped 3 to 10 different measurements into a single  $s$  bin, as indicated in Table I. From each measurement,  $i$ , we obtained the experimental slope,  $b_i$ , and the experimental error in this slope,  $\Delta_i$ . These are shown in Figs. 2 and 3. We then calculated  $b(s)$ , the average of the  $n$  values of  $b_i$  in each  $s$  bin, from

$$b(s) = \frac{\sum_{i=1}^n b_i / (\Delta_i)^2}{\sum_{i=1}^n (1/\Delta_i)^2}. \quad (12)$$

We took  $s$  to be the unweighted average of the  $n$  values of  $s_i$  in each bin. There are two ways of estimating the error in each  $b(s)$ . One is to assume that the errors quoted by the experimenters

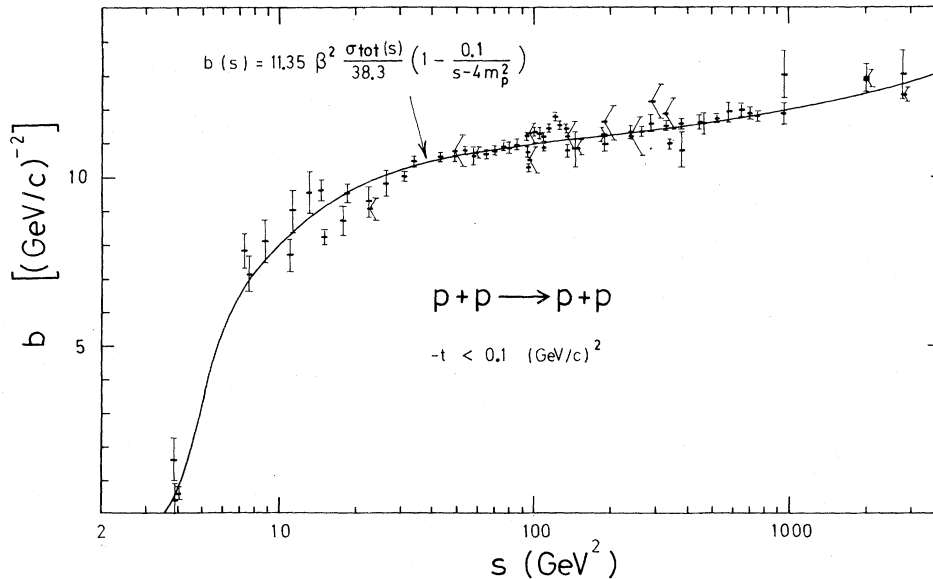


FIG. 2. The measured slope,  $b$  in  $e^{-b|t|}$ , is plotted against  $s$  for proton-proton elastic scattering at  $-t < 0.1 \text{ (GeV/c)}^2$ . Also plotted is Eq. (11). The references at different  $s$  values are indicated in Table I.

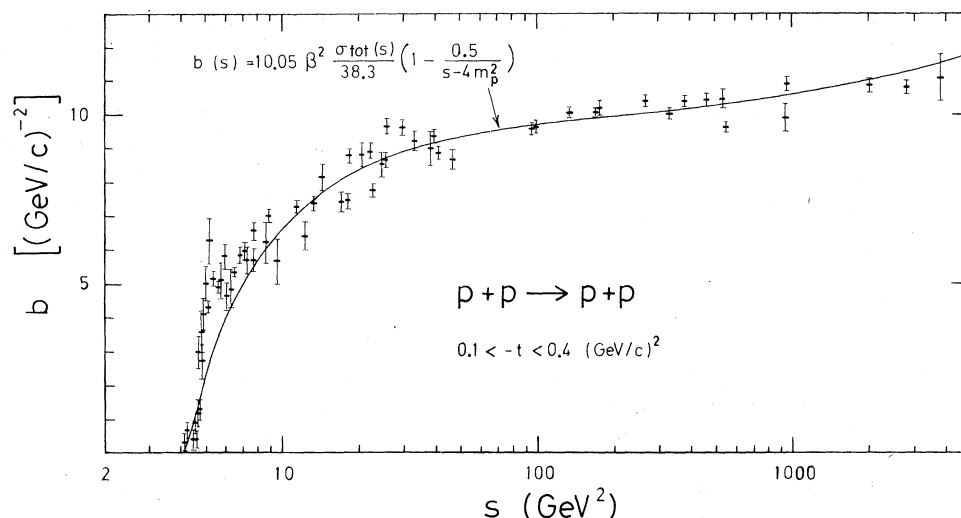


FIG. 3. The measured slope,  $b$  in  $e^{-b|t|}$ , is plotted against  $s$  for proton-proton elastic scattering at  $0.1 < -t < 0.4$   $(\text{GeV}/c)^2$ . Also plotted is Eq. (11). The references at different  $s$  values are indicated in Table I.

TABLE I. The averaged values of the measured slope  $b(s)$  for proton-proton elastic scattering are listed for different  $s$  bins with average value  $s$ . The value of  $b$  at each  $s$  is calculated from Eq. (11) using  $\sigma_{\text{tot}}/38.3$  mb from Fig. 1.

$ t $ $(\text{GeV}/c)^2$	$s_{\text{min}}$ $(\text{GeV})^2$	$s_{\text{max}}$ $(\text{GeV})^2$	Number of measurements	References	$s$ $(\text{GeV}^2)$	$b(s) \pm \Delta(s)$ $[(\text{GeV}/c)^{-2}]$	$\frac{\sigma_{\text{tot}}}{38.3 \text{ mb}}$	$b_{\text{calc}}(s)$ $[(\text{GeV}/c)^{-2}]$	$\chi^2$
<0.1	3.85	4.01	3	31,32	3.94	$0.66 \pm 0.20$	$0.585 \pm 0.010$	$0.54 \pm 0.17$	0.21
	7.4	11.0	4	33,34	8.7	$7.64 \pm 0.18$	$1.164 \pm 0.012$	$7.72 \pm 0.08$	0.17
	11.3	17.8	5	33,34,35,36	14.5	$8.71 \pm 0.23$	$1.057 \pm 0.005$	$9.00 \pm 0.05$	1.52
	18	31	5	33,36,37	24	$9.77 \pm 0.13$	$1.034 \pm 0.005$	$9.97 \pm 0.05$	2.06
	37	49	4	36,37	44	$10.56 \pm 0.05$	$1.013 \pm 0.005$	$10.55 \pm 0.05$	0.02
	54	70	5	37,38	61	$10.72 \pm 0.04$	$1.005 \pm 0.005$	$10.73 \pm 0.05$	0.02
	76	86	3	37	81	$10.91 \pm 0.04$	$1.003 \pm 0.005$	$10.88 \pm 0.05$	0.22
	94	108	8	36,37,38,39	99	$10.99 \pm 0.10$	$1.001 \pm 0.005$	$10.95 \pm 0.06$	0.12
	110	148	9	36,37,38,39	130	$11.20 \pm 0.10$	$1.002 \pm 0.005$	$11.06 \pm 0.06$	1.44
	190	192	3	36,39	191	$11.18 \pm 0.11$	$1.004 \pm 0.005$	$11.18 \pm 0.06$	0.00
	225	280	5	36,39	257	$11.38 \pm 0.10$	$1.008 \pm 0.005$	$11.28 \pm 0.06$	0.74
	306	380	5	36,39	347	$11.41 \pm 0.10$	$1.016 \pm 0.005$	$11.41 \pm 0.06$	0.00
	446	462	2	36,40	454	$11.60 \pm 0.11$	$1.023 \pm 0.005$	$11.52 \pm 0.06$	0.41
	504	695	4	36	608	$11.80 \pm 0.07$	$1.034 \pm 0.015$	$11.67 \pm 0.18$	0.45
	750	960	3	36,40,41	886	$11.83 \pm 0.15$	$1.047 \pm 0.015$	$11.84 \pm 0.18$	0.00
	2000	2808	4	40,41	2405	$12.68 \pm 0.14$	$1.114 \pm 0.017$	$12.63 \pm 0.19$	0.05
									$\Sigma = 7.43$
0.1-0.4	4.13	4.30	3	42,43	4.23	$0.46 \pm 0.18$	$0.629 \pm 0.010$	$0.32 \pm 0.10$	0.46
	4.40	5.00	10	42,43,44	4.67	$1.87 \pm 0.35$	$1.060 \pm 0.015$	$1.49 \pm 0.20$	0.89
	5.08	6.33	9	42,43,45,46	5.71	$5.02 \pm 0.11$	$1.238 \pm 0.020$	$3.68 \pm 0.25$	24.07
	6.77	7.66	5	34,43,45	7.28	$5.95 \pm 0.24$	$1.178 \pm 0.010$	$5.31 \pm 0.17$	4.74
	8.56	9.47	3	34,45,47	8.95	$6.82 \pm 0.24$	$1.115 \pm 0.010$	$6.17 \pm 0.14$	5.47
	11.3	14.3	4	34,48,49	12.8	$7.30 \pm 0.18$	$1.066 \pm 0.005$	$7.35 \pm 0.10$	0.06
	17.1	22.1	5	50,51,52,53	19.2	$8.20 \pm 0.26$	$1.043 \pm 0.005$	$8.29 \pm 0.08$	0.11
	22.4	25.8	4	51,52,53	24.4	$8.61 \pm 0.31$	$1.031 \pm 0.005$	$8.65 \pm 0.06$	0.02
	29.6	46.8	6	16,52,53	37.9	$9.09 \pm 0.13$	$1.019 \pm 0.005$	$9.16 \pm 0.05$	0.05
	95.7	133	3	39,54	108	$9.71 \pm 0.10$	$1.000 \pm 0.005$	$9.67 \pm 0.05$	0.13
	170	330	4	39,54	234	$10.13 \pm 0.07$	$1.013 \pm 0.005$	$10.00 \pm 0.05$	2.28
	377	552	4	40,54,55,56	480	$10.12 \pm 0.17$	$1.023 \pm 0.005$	$10.20 \pm 0.05$	0.20
	930	2013	3	40,56	1279	$10.74 \pm 0.19$	$1.073 \pm 0.015$	$10.75 \pm 0.16$	0.00
	2808	3844	2	40,55	3326	$10.82 \pm 0.14$	$1.137 \pm 0.017$	$11.42 \pm 0.17$	3.30
									$\Sigma = 41.78$

are exactly correct and to take

$$\Delta'(s) = \frac{1}{\left[ \sum_{i=1}^n (1/\Delta_i^2) \right]^{1/2}}. \quad (13)$$

Another way is to average the deviations of each  $b_i$  from the average value  $b(s)$

$$\Delta^*(s) = \left\{ \frac{\sum_{i=1}^n [b_i - b(s)]^2 / \Delta_i^2}{(n-1) \sum_{i=1}^n (1/\Delta_i^2)} \right\}^{1/2}. \quad (14)$$

The correctness of using  $\Delta'$  or  $\Delta^*$  depends on each experimenter's accuracy in estimating his systematic errors. This clearly may vary from experiment to experiment and there is no objective way to judge this. Therefore we took the error in  $b(s)$  to be the average of  $\Delta'$  and  $\Delta^*$  for each  $s$  bin

$$\Delta(s) = \left( \frac{1}{2} [\Delta'(s)^2 + \Delta^*(s)^2] \right)^{1/2}. \quad (15)$$

We believe that this gives a fair estimate of the true uncertainty in  $b(s)$  for each bin. The values of  $b(s)$  and  $\Delta(s)$  are listed in Table I along with information about the experiments from which they were obtained. They are listed for both  $t$  ranges in the diffraction peak. These slopes are plotted in Fig. 4 against  $s$  along with the prediction of Eq. (11).

The excellent agreement of the model with the measured slopes is now quite clear. The averaging procedure has removed many of the experi-

mental fluctuations seen in Figs. 2 and 3. In Fig. 4 one can see that Eq. (11) agrees with the data in both  $t$  regions of the diffraction peak at all energies from  $s = 4m_p^2$  to  $4000$   $(\text{GeV}/c)^2$ . The value of Eq. (11) for each  $s$  bin is given in Table I. Also shown is the  $\chi^2$  for each  $s$  bin and the total  $\chi^2$  for each  $t$  region. In calculating the uncertainty in  $b_{\text{calc}}(s)$  we included the estimated error in  $\sigma_{\text{tot}}(s)$  indicated in Table I and an uncertainty of  $\pm 0.2 \langle t \rangle$  in  $\langle t \rangle$ . In the  $0.1 < |t| < 0.4$   $(\text{GeV}/c)^2$  region  $\chi^2$  is 41.8 for 14 points, which is somewhat high, but 24.1 of this comes from one very low  $s$  point. There does seem to be a 10–20% deviation near  $s = 6$   $(\text{GeV})^2$ . In this large- $t$  region the relation between  $t$  and  $P_{\perp}^2$  given by Eq. (9) is very sensitive to the value of  $\langle t \rangle$ . A more likely problem is that particle-identity effects<sup>6</sup> are not negligible at  $-t = 0.4$   $(\text{GeV}/c)^2$  since that is not so far from  $90^\circ$  at  $s = 6$   $(\text{GeV})^2$ . In the small- $t$  region both effects become negligible at a much lower  $s$  and the  $\chi^2$  is 7.4 for 16 points.<sup>57</sup> This is more than acceptable since there is only one free parameter, the radius.

Plotting the slope against  $s$  is probably the most precise way to demonstrate numerically the quality of the fit. However, it may be even more interesting to demonstrate that the experimental differential cross sections are totally independent of energy when we plot

$$\frac{d\sigma/dt}{\sigma_{\text{tot}}^2(s)/16\pi} \text{ against } \beta^2 P_{\perp}^2 \frac{\sigma_{\text{tot}}(s)}{38.3 \text{ mb}} \quad (16)$$

as suggested by Eq. (4). This avoids the kinematic

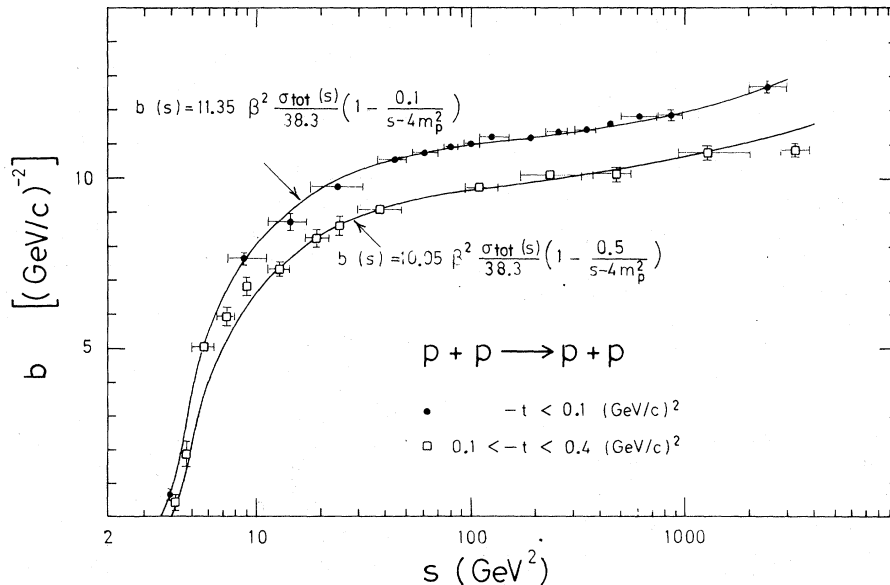


FIG. 4. The averaged value of the measured slope,  $b$  in  $e^{-b|t|}$ , is plotted against  $s$  for proton-proton elastic scattering in both  $t$  regions of the diffraction peak. Equation (11) is also plotted for both regions. The references at each  $s$  value are given in Table I.

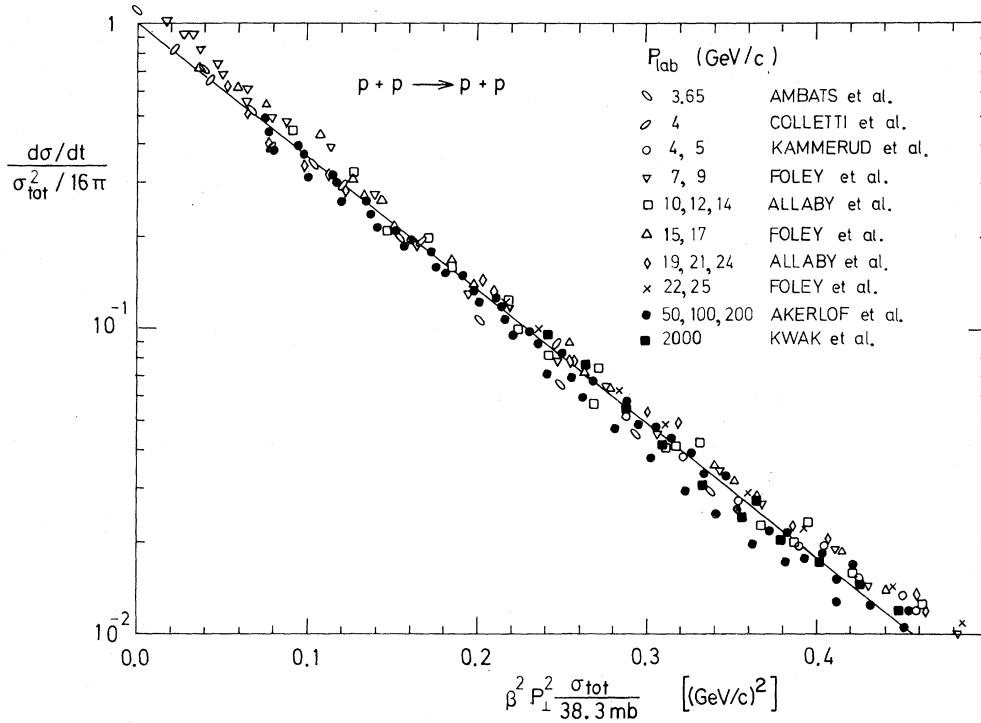


FIG. 5. The measured (Refs. 16, 34, 45, 47, 52–55) proton-proton elastic differential cross section  $d\sigma/dt$  divided by  $[\sigma_{\text{tot}}(s)]^2/16\pi$  is plotted against  $\beta^2 P_{\perp}^2 \sigma_{\text{tot}}(s)/38.3$ . At each  $s$  value  $\sigma_{\text{tot}}(s)$  is taken from Fig. 1. The line shown is  $\exp(-10.05 \beta^2 P_{\perp}^2 \sigma_{\text{tot}}/38.3)$ .

contortions of transforming from  $t$  to  $\rho_{\perp}^2$  and the corresponding  $1 - 2\langle t \rangle / (s - 4m^2)$  term. In Fig. 5 we have plotted a variety of  $P_{\text{lab}}$  values as indicated. To avoid crowding we have not plotted all available data; but have chosen a sample of widely varying energies and used the measurements with small errors whenever possible. There are clearly some normalization differences between different experiments but they are surprisingly small. As might be expected from our knowledge of Fig. 4, the fit in Fig. 5 is excellent. The data below 3.5 GeV/c begins to deviate at large  $\rho_{\perp}^2$ , possibly because of  $90^\circ$  particle-identity effects. But the data shown from  $P_{\text{lab}}$  of 3.65 to 2000 GeV/c has no observable energy dependence. All variations seem to be experimental fluctuations independent of  $P_{\text{lab}}$ . Thus the  $p$ - $p$  elastic diffraction cross section appears to be a single universal function of the variable  $\beta^2 P_{\perp}^2 \sigma_{\text{tot}}(s)/38.3$ .

One should notice that Fig. 5 is a rather expanded graph which gives a very sensitive test of universality. This sensitivity can be best demonstrated by plotting a selection of the same data against the variable suggested in the "geometrical scaling" model,<sup>19</sup>  $t\sigma_{\text{tot}}(s)/38.3$ . This is plotted in Fig. 6. This figure clearly shows that while the variation in  $\sigma_{\text{tot}}(s)$  removes some of the energy dependence at high  $P_{\text{lab}}$ , it does not result in a

universal energy-independent curve.

Since the variable  $\beta^2 P_{\perp}^2 \sigma_{\text{tot}}(s)/38.3$  does appear to lead to a universal energy-independent curve for proton-proton elastic diffraction scattering, it might be useful to discuss why this variable was originally suggested.<sup>2, 6, 7, 12</sup>

The Lorentz-contracted geometrical model assumes that when two protons collide, the elastic scattering cross section is determined by the "interaction probability density"  $\rho(\vec{R})$ . This  $\rho(\vec{R})$  depends on  $\vec{R}$ , the distance between the two protons at the instant they interact. In some sense  $\rho(\vec{R})$  is similar to a potential, but it is defined by the fact that its Fourier transform is exactly the elastic scattering amplitude

$$\frac{d\sigma/dt}{(d\sigma/dt)_0} \propto |f(\vec{P})|^2 = \left| \int d^3R e^{i\vec{P} \cdot \vec{R}} \rho(\vec{R}) \right|^2. \quad (17)$$

The scattering amplitude is sometimes assumed to be proportional to the product of the densities of the "stuff" in each of the two protons.<sup>58</sup> Here we assume that a proton has a structure function  $\phi(\vec{r})$  which depends on  $\vec{r}$ , the distance from its own center. We also assume that  $\rho(\vec{R})$  is obtained by folding together the two  $\phi(\vec{r})$  functions.

$$\rho(\vec{R}) = \int d^3R' \phi(\vec{R}' - \vec{R}/2) \phi(\vec{R}' + \vec{R}/2). \quad (18)$$

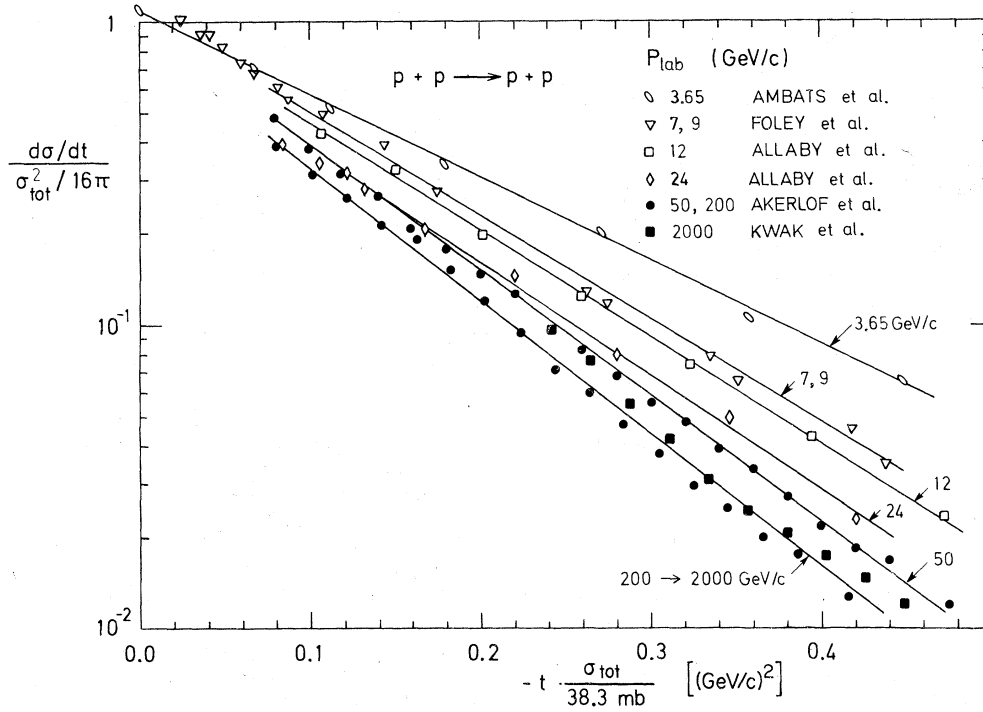


FIG. 6. Some of the measured (Refs. 34, 52–55) proton-proton elastic differential cross sections are plotted against the geometric scaling variable  $-t\sigma_{\text{tot}}(s)/38.3$ .

The function  $\phi(\vec{r})$  describes the shape of each proton as measured by the  $p$ - $p$  elastic scattering cross section. We assume that in its own rest frame each proton is a Gaussian sphere of radius  $A'$ .

$$\phi(\vec{r}) \propto e^{-(x^2+y^2+z^2)/A'^2}. \quad (19)$$

In the c.m. system, where the interaction occurs, the Lorentz contraction squashes down each sphere by a factor  $\gamma = E_{\text{c.m.}}/m_p$  in the direction of motion,  $z^*$ . Then  $\phi(\vec{r})$  in the c.m. is given by

$$\phi(\vec{r}) = \frac{\gamma}{(\pi A'^2)^{3/2}} \exp\left[-\frac{x^2+y^2}{A'^2} - \frac{z^2}{(A'/\gamma)^2}\right]. \quad (20)$$

The normalization is chosen so that

$$\int d^3r \phi(r) = 1. \quad (21)$$

The interaction probability density  $\rho(\vec{R})$  is obtained by substituting (20) into (18) and integrating. This gives

$$\rho(\vec{R}) = \frac{\gamma}{(\pi A'^2)^{3/2}} \exp\left[-\frac{X^2+Y^2}{2A'^2} - \frac{Z^2}{2(A'/\gamma)^2}\right]. \quad (22)$$

The Fourier transform of  $\rho(\vec{R})$  is defined by Eq. (17) to be the elastic scattering amplitude  $f(\vec{P})$ .

$$\begin{aligned} f(\vec{P}) &= \int d^3R e^{i\vec{P}\cdot\vec{R}} \rho(\vec{R}) \\ &= \exp\left[-\frac{1}{2}A'^2(P_1^2 + P_{\parallel}^2/\gamma^2)\right]. \end{aligned} \quad (23)$$

For  $p$ - $p$  elastic scattering in the c.m. the following simple kinematic relations hold:

$$\begin{aligned} P_{\parallel}^2 &= P^2 - P_{\perp}^2, \\ \beta^2 &= 1 - 1/\gamma^2, \\ P^2 &= \beta^2 \gamma^2 m_p^2, \end{aligned} \quad (24)$$

where  $m_p$  is the proton mass. Using them we can write the elastic amplitude as

$$f(\vec{P}) = e^{-A'^2(\beta^2 P_{\perp}^2 - \beta^2 m_p^2)/2}. \quad (25)$$

The elastic cross section is then given by Eq. (17) to be

$$\frac{d\sigma}{dt} = \left(\frac{d\sigma}{dt}\right)_0 e^{-A'^2\beta^2 P_{\perp}^2}. \quad (26)$$

The  $\beta^2 m_p^2$  term has no angular dependence and was therefore absorbed into  $(d\sigma/dt)_0$ , whose  $s$  dependence we do not predict.

Finally we assume that the energy dependence of  $\sigma_{\text{tot}}$  is caused by the proton radius  $A'$  increasing with energy. If we define  $A$  to be the proton radius at some energy  $s_0$ , where  $\sigma_{\text{tot}}$  has the value  $\sigma_{\text{tot}}(s_0)$ , then the radius at another energy  $s$  is given by

$$A'^2 = A^2 \frac{\sigma_{\text{tot}}(s)}{\sigma_{\text{tot}}(s_0)}. \quad (27)$$

The cross section then has the form

$$\frac{d\sigma}{dt} = \frac{\sigma_{\text{tot}}^2(s)}{16\pi} \exp \left[ -A^2 \beta^2 P_1^2 \frac{\sigma_{\text{tot}}(s)}{\sigma_{\text{tot}}(s_0)} \right], \quad (28)$$

where  $A$  is an energy-independent radius parameter.

Thus using a very simple geometrical model we easily derived a universal formula which fits all the measured  $p$ - $p$  elastic diffraction cross sections. The quality of the fit in the diffraction peak strongly suggests that the Lorentz-contracted

geometrical model must contain a core of truth. Then the variable  $\beta^2 P_1^2 \sigma_{\text{tot}}(s)/38.3$  should also be useful for large- $t$  data. Plotting the large-angle data against this variable does remove much of the energy dependence but it does not remove it all.<sup>6,17</sup> Obtaining an exact fit at large angles will probably require an exact knowledge of particle-identity effects.<sup>6</sup> This will require either measuring the  $p$ - $p$  spin dependence near  $90^\circ$  or trying to guess its nature.

\*On leave from Randall Lab. of Physics, University of Michigan, Ann Arbor, Michigan 48109.

<sup>1</sup>R. Serber, Phys. Rev. Lett. **10**, 357 (1963); Rev. Mod. Phys. **36**, 649 (1964).

<sup>2</sup>A. D. Krisch, Phys. Rev. Lett. **11**, 217 (1963); Phys. Rev. **135**, B1456 (1964).

<sup>3</sup>L. Van Hove, Nuovo Cimento **28**, 798 (1963); Rev. Mod. Phys. **36**, 655 (1964).

<sup>4</sup>T. T. Wu and C. N. Yang, Phys. Rev. **137**, B708 (1965).

<sup>5</sup>L. Durand and R. Lipes, Phys. Rev. Lett. **20**, 637 (1968).

<sup>6</sup>A. D. Krisch, in *Lectures in Theoretical Physics*, edited by W. E. Brittin *et al.* (Univ. of Colorado Press, Boulder, 1966), Vol. IX, p. 1; Phys. Rev. Lett. **19**, 1149 (1967).

<sup>7</sup>A. D. Krisch, in *Proceedings of the Canadian Institute of Particle Physics Summer School, McGill University, 1972*, edited by R. Henei and B. Margolis (McGill Univ. Press, Montreal, 1973).

<sup>8</sup>K. Huang, Phys. Rev. **156**, 1555 (1967).

<sup>9</sup>C. N. Yang *et al.*, Phys. Rev. **188**, 2159 (1969); Phys. Rev. Lett. **25**, 1072 (1970).

<sup>10</sup>R. P. Feynman, Phys. Rev. Lett. **23**, 1415 (1969); and private communication.

<sup>11</sup>H. I. Miettinen, Acta Phys. Pol. **B6**, 625 (1975) and references contained therein.

<sup>12</sup>A. D. Krisch, Phys. Lett. **44B**, 71 (1973).

<sup>13</sup>E. Leader and M. R. Pennington, Phys. Rev. Lett. **27**, 1325 (1971).

<sup>14</sup>S. Barshay and Y. A. Chao, Phys. Lett. **38B**, 225 (1972); **38B**, 229 (1972); J. S. Ball and S. S. Pinsky, Phys. Rev. Lett. **27**, 1820 (1971).

<sup>15</sup>A. C. Mellissinos and S. L. Olson, Phys. Lett. **17C**, 77 (1975).

<sup>16</sup>J. Allaby *et al.*, in *Proceedings of the Topical Conference on High Energy Collisions of Hadrons, CERN, 1968* (CERN, Geneva, 1968), p. 580.

<sup>17</sup>G. Giacomelli, Phys. Lett. **23C**, 123 (1975).

<sup>18</sup>K. Abe *et al.*, Phys. Lett. **63B**, 239 (1976).

<sup>19</sup>J. Dias de Deus *et al.*, Nucl. Phys. **B59**, 231 (1973); **B71**, 481 (1974); Acta Phys. Pol. **B6**, 613 (1975).

<sup>20</sup>D. V. Bugg *et al.*, Phys. Rev. **146**, 980 (1966).

<sup>21</sup>K. J. Foley *et al.*, Phys. Rev. Lett. **19**, 857 (1967).

<sup>22</sup>S. P. Denisov *et al.*, Phys. Lett. **36B**, 415 (1971).

<sup>23</sup>A. S. Carroll *et al.*, Phys. Lett. **61B**, 303 (1976).

<sup>24</sup>K. Eggert *et al.*, Contribution No. G1-38 to the European Physical Society International Conference, Palermo, 1975 (unpublished).

<sup>25</sup>S. R. Amendolia *et al.*, Phys. Lett. **44B**, 119 (1973).

<sup>26</sup>U. Amaldi *et al.*, Phys. Lett. **44B**, 112 (1973).

<sup>27</sup>R. A. Carrigan, Phys. Rev. Lett. **24**, 168 (1970).

<sup>28</sup>Whenever the experimenters or compilation quoted a slope in the correct  $t$  range we used their value. When they quoted only cross sections we used them to calculate the slope with the standard equation in the UCRL compilation (Ref. 29).

<sup>29</sup>O. Benary, L. R. Price, and G. Alexander, UCRL Report No. UCRL-20000 NN, 1970 (unpublished).

<sup>30</sup>T. Lasinski *et al.*, Nucl. Phys. **B37**, 1 (1972); Phys. Rev. **179**, 1426 (1969).

<sup>31</sup>O. Chamberlain *et al.*, Phys. Rev. **103**, 1860 (1956).

<sup>32</sup>O. A. Towler *et al.*, Phys. Rev. **85**, 1024 (1952).

<sup>33</sup>N. Dalkhazhav *et al.*, Yad. Fiz. **8**, 342 (1968) [Sov. J. Nucl. Phys. **8**, 196 (1969)].

<sup>34</sup>I. Ambats *et al.*, Phys. Rev. **D9**, 1179 (1974).

<sup>35</sup>C. Clyde, thesis, UCRL Report No. UCRL-20001, 1970 (unpublished).

<sup>36</sup>V. Bartenev *et al.*, Phys. Rev. Lett. **29**, 1755 (1972); **31**, 1088 (1973).

<sup>37</sup>G. G. Bezogikh *et al.*, Phys. Lett. **30B**, 274 (1969).

<sup>38</sup>I. M. Geshkov *et al.*, Phys. Rev. **D13**, 1846 (1976).

<sup>39</sup>D. Ayres *et al.*, Phys. Rev. Lett. **35**, 1195 (1975).

<sup>40</sup>G. Barbiellini *et al.*, Phys. Lett. **39B**, 663 (1972).

<sup>41</sup>U. Amaldi *et al.*, Phys. Lett. **36B**, 504 (1971).

<sup>42</sup>D. Ryan *et al.*, Penn-Princeton Accelerator Report No. PPAR 11, 1969 (unpublished).

<sup>43</sup>M. G. Albrow *et al.*, Nucl. Phys. **B23**, 445 (1970).

<sup>44</sup>M. G. Mesčerjakov *et al.*, Nuovo Cimento Suppl. **3**, 119 (1956).

<sup>45</sup>R. C. Kammerud *et al.*, Phys. Rev. **D4**, 1309 (1971).

<sup>46</sup>A. M. Eisner *et al.*, Phys. Rev. **138**, 670B (1965).

<sup>47</sup>S. Coletti *et al.*, Nuovo Cimento **49A**, 479 (1966).

<sup>48</sup>G. Alexander *et al.*, Phys. Rev. **173**, 1322 (1968).

<sup>49</sup>E. Colton *et al.*, UCLA Report No. UCLA-1025, 1968 (unpublished).

<sup>50</sup>J. Ginestet *et al.*, Nucl. Phys. **B13**, 283 (1969).

<sup>51</sup>D. Harting *et al.*, Nuovo Cimento **38**, 60 (1965).

<sup>52</sup>K. J. Foley *et al.*, Phys. Rev. Lett. **11**, 425 (1963); **15**, 45 (1965); Phys. Rev. **181**, 1775 (1969).

<sup>53</sup>J. V. Allaby *et al.*, Nucl. Phys. **B52**, 316 (1973).

<sup>54</sup>C. W. Akerlof *et al.*, Phys. Rev. Lett. **35**, 1406 (1975); Phys. Lett. **59B**, 197 (1975).

<sup>55</sup>N. Kwak *et al.*, Phys. Lett. **58B**, 233 (1975).

<sup>56</sup>A. Böhm *et al.*, Phys. Lett. **49B**, 491 (1974).

<sup>57</sup>After completing the figures and table we discovered another experiment at  $|t| < 0.1$  (GeV/c)<sup>2</sup> with 26 measurements in the range  $s = 7.3$ –133 (GeV)<sup>2</sup> by G. G. Bezogikh *et al.*, Phys. Lett. **43B**, 85 (1973). Rather than redo the figures and table we decided to numerically compare each measured slope with  $b_{\text{calc}}$  from



Eq. (11). The agreement is excellent. Adding their quoted statistical and systematic errors in quadrature we found a  $\chi^2$  of 16.2 for 26 points. While this agreement alone is quite significant, it is not as significant as the  $\chi^2$  in Table I because each point in Table I contains many experimental points and thus has smaller errors, typically  $\pm 0.1$  (GeV/c)<sup>2</sup> compared with  $\pm 0.3$  for Bezogikh *et al.* alone. The significance of a fit depends not only on  $\chi^2$  but also on the smallness of the errors. Our late discovery of this data points out

that there may be other important undiscovered data.

<sup>58</sup>The idea that the cross section was proportional to the product of the material in the two incident particles was perhaps first suggested by W. Heisenberg, Z. Phys. 101, 533 (1936); 113, 61 (1939); 126, 569 (1949); 133, 65 (1952). The idea has been developed further by N. Byers and C. N. Yang, Phys. Rev. 142, 976 (1966); and T. T. Chou and C. N. Yang, Phys. Rev. Lett. 20, 1213 (1968). It has also been studied by H. J. Bhabha, Proc. R. Soc. London A219, 293 (1963).